INTERNATIONAL JOURNAL OF AUTOMOTIVE AND MECHANICAL ENGINEERING (IJAME)
ISSN: 2229-8649 e-ISSN: 2180-1606
VOL. 18, ISSUE 3, 8882 – 8894
DOI: https://doi.org/10.15282/ijame.18.3.2021.04.0681

ORIGINAL ARTICLE

Numerical Analysis of Thick Isotropic and Transversely Isotropic Plates in Bending using FE Based New Inverse Shear Deformation Theory

D.P. Bhaskar[1*], A.G.Thakur[2], I.I. Sayyad[1] and S.V. Bhaskar[1]

[1]Department of Mechanical Engineering, Sanjivani College of Engineering Kopargaon-423601, SP Pune University, M.S., India
[2]Sanjivani College of Engineering Kopargaon-423601, SP Pune University, M.S., India

ABSTRACT – In this work, using the new inverse trigonometric kinematic displacement function, the bending solution of simply supported isotropic and transversely isotropic thin, moderately thin and thick square plates with aspect ratio variations is given. The paper introduces a new inverse trigonometric shear deformation theory (nITSDT) for the bi-directional bending study, which is variationally compatible. The transverse shear stress can be obtained directly from the constitutive relationships on the top and bottom surfaces of the plate that satisfy the shear stress-free surface conditions, so the theory does not need a factor for shear correction. The dynamic version of the virtual work principle is used to obtain the governing equations and boundary conditions of the theory. The finite element solution has been developed using MATLAB code based on the present theory for simply supported laminated composite plates. In order to illustrate the efficiency of the proposed theory, the results of displacements and stresses are compared with those of other refined theories and exact solutions. The findings obtained from the use of the theory are found to agree well with the precise results of elasticity.

ARTICLE HISTORY
Received: 23rd March 2021
Revised: 20th Aug 2021
Accepted: 3rd Sept 2021

KEYWORDS
Shear deformation;
Transversely isotropic;
Transverse shear stresses;
FEM;
MATLAB

INTRODUCTION

Isotropic plates are utilised as structural elements in a variety of applications, including mechanical and civil engineering. Plates are under transverse loading bend in most engineering structures, such as long spans, walkways, and platforms. As a consequence, the structural design of the model is based on the analysis of the bends in these plates, and this region has received a lot of attention. A growing quantity of research has been devoted to the study of thin rectangular plates of uniform thickness over the last few decades, principally based on the classical plate theory, CPT. [1]. It is based on the theory that, after deformation, straight lines normal to the mid-surface retain straight. The transverse shear and transverse normal strains are both zero according to the CPT's kinematic assumptions. Subsequently, CPT neglects transverse shear deformation, where the effects of shear deformation are more significant. Thus, its appropriateness is restricted only to thin plates. Mindlin's Shear Deformation of First Order, FSDT is regarded as a CPT's improvement. It is based on the theory that the normal to the un-deformed mid-plane stays straight but not necessarily normal to the mid-plane after deformation, and the displacement field through the thickness for the in-plane displacement is in linear nature. FSDT is based on stresses developed [2], which combines shear influence and the displacement-based approach [3]. For transversely isotropic plates, a consistent second-order plate theory is derived. Analytically, the theory is validated against three-dimensional elasticity theory [4]. In FSDT, the variation of transverse-shear stresses and strains is adjusted by including the shear correction factor (SCF). Many higher-order shear deformation theories (HSDTs) are developed by eliminating the use of SCF to achieve practical variations in transverse-shear strains and stresses via the direction of thickening. Inside a given HSDT [5], parabolic distribution shear stress is accomplished via the thickness of the constant thickness layers.

The comprehensive reviews of various refined theories [6] and a new hypothesis for the plate are used for thick plate vibration study through the thickness of the plate. The material properties fluctuate according to the power-law distribution [7], and the concept of virtual work is employed to derive the governing equations and model parameters in this theory. Navier's solution approach is used to solve simply supported curvature in elevation beams. Using Reissner's Mixed Variational Theory (RMVT), the author [8] has constructed and tested mixed LW and ESL plate and shell structures that can fully satisfy C^0s- requirements. Newer reviews on plate bending have been submitted and presented [9]. Plenty of problems are solved using trigonometric shear deformation theory [10] and the analytical approach. The effect of transverse-shear and normal strain on isotropic stresses in static bending has been investigated for thick plates. For the static flexure and free vibration study of isotropic plates, two variable refined plate theories were developed [11], and this theory produces frequencies similar to those of the theory of FSDT. Employing two modified Vlasov foundation models [12], the effect of soil variability on the bending of circular thin plates is investigated. Several refined shell methods [13] were used to assess the static and free vibrations of composite laminates and sandwiched geometrical shapes. The exponential shear deformation theory was introduced [13], which later proposed for multilayered beam structures.

*CORRESPONDING AUTHOR | D.P. Bhaskar | ✉ bhaskardhirajmech@sanjivani.org.in

For the bidirectional bending of plates (provided an exact elasticity solution [14]), effective vibration analysis of thick rectangular homogeneous plates[15] was carried out.

The influence of transversely-shear and normal deformation on thermal-mechanical analyses of FG plates was investigated, and the results were shown to be valuable as a benchmark [16]. A theory of fifth-order shear deformation considering transverse shear deformation effect as well as transverse normal strain deformation effect was proposed [17] for static flexure analysis of simply supported isotropic plates. A sixth-order differential equations system has been developed [18], and analyses of elastic plates lead to two boundary conditions. 3D elasticity equations of plates on the foundations of Pasternak are considered in the formulation of the plate [19]. The exact solution is given on a two-parameter basis by the displacement potential functions of a simply supported rectangular plate with constant yet arbitrary thickness. The assumptions of variance of Young's moduli (E) and shear moduli (G) [20] through the plates' thickness of plate has been examined. The strategy utilises displacement-based potential functions for transversely isotropic plates and 3-D elasticity solutions established. The bending behaviour of transversely isotropic rectangular plates with different thicknesses was critically studied [21]. For fulfilment, governing-differential equations are solved using the division of variables system, as well as accurate plate boundary conditions. Using novel kinematic functions bending analyses of laminated composite plates were carried out for uniformly distributed, and sinusoidal loadings [22-23], in which different aspect rations were considered and FE formulation for these problems were devised.

The modified computer model introduced [24] for the thermal analysis of composite laminates and sandwiches plates takes into account the impacts of shear and normal deflections. The numerical solution technique is based on MATLAB [25], the symbolic codes are written, and similar types of code are used in the present study also. Several research papers are provided in the studies review static, dynamic, and buckling behaviour of plates and shells under thermal and mechanical loading conditions [25-26]. A finite element analysis [27] was proposed for the static/dynamic analysis of FG plates with cylindrical shells based on higher-order approximation. The bending behaviour of laminated and sandwich shells [28-30] was studied with thermo-mechanical load using Carrera's unified solution. The different shear deformation models [31] were used to analyse the thermo-elastic bends of composite laminates. A simplified and accurate plate theory taking account for transverse normal strain is offered [12, 16 and 33]. The numerical solution technique is based on MATLAB[32], the symbolic codes are written, and similar types of code are used in the present study.

The present work proposes a displacement-based new inverse trigonometric shear deformation theory (nITSDT) for bi-directional bending and assessment of thick isotropic and transversely isotropic plates, which takes into account the effects of transverse shear deformation and rotating inertia. MATLAB code developed based on FE formulation for this new theory. For the rapid generation of stiffness matrices and to minimise numerical instabilities, symbolic computation has been used primarily with FE formulation. For the bending-analyses of isotropic/transversely isotropic plates, the demonstrated theory was found to be modest and effective.

MATHEMATICAL FORMULATION

In the coordinate scheme x-y-z, the isotropic plate presented in Figure 1 has dimensions (a×b×h). The plate boundaries correspond per the x:0-a and y:0-b. A transverse load applied to the plate is of SDL and UDL on the plate's upper surface.

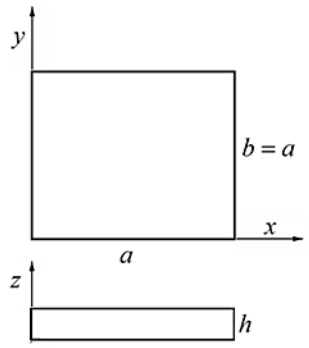

Figure 1. Schematic diagram of a square plate**.**

Displacement Fields and Associated Strain Terms

Equation (1) presents the axial-displacements u and v in the x and y-directions, one-to-one, then the transverse-displacement:w in conjunction with the z:direction at all points in the entire plate and written in the functional-form, according to nITSDT.

$$u = u_0 + u_b + u_s, v = v_0 + v_b + v_s \; and \; w = w_0 \tag{1}$$

where u_0, v_0 and w_0 are the mid-pane displacements,$u_b$and v_b are the bending components of deformations and u_s and v_s are the shear components of deformations. The bending components are represented as $u_b = -z\frac{(\partial w_0}{\partial x)}$ & $v_b = -z\frac{(\partial w_0}{\partial y)}$. The shear components are represented as $u_s = \phi f(z)$ & $v_s = \psi f(z)$, whereas the $f(z)$, novel kinematic shape-

function regulates the deviation of shear stress transversely through the plate's depth and ϕ, ψ being transverse normal rotation components about y and x axes consistently. When u_0, v_0, w_0, *"*u_0, v_0, w_0, ϕ and ψ" are recognised, the displacements *"*u, v and w" at arbitrary points in the plate are calculated. The in-plane and transverse-shear strains, by way of indicated by Eq. (2), characterise the state-of-strains at an arbitrary location in the plate.

$$\begin{Bmatrix} \varepsilon_x \\ \varepsilon_y \\ \gamma_{xy} \\ \gamma_{zx} \\ \gamma_{yz} \end{Bmatrix} = \begin{pmatrix} \dfrac{(\partial u_0}{\partial x) - z\dfrac{(\partial^2 w_0}{\partial x^2) + \dfrac{f(z)(d\phi}{\partial x)}} \\ \dfrac{(\partial v_0}{\partial y) - z\dfrac{(\partial^2 w_0}{\partial y^2) + \dfrac{f(z)(d\psi}{\partial x)}} \\ \dfrac{(\partial u_0}{\partial y) + \dfrac{(\partial v_0}{\partial x) - 2z\left(\dfrac{\partial^2 w_0}{\partial x \partial y}\right) + f(z)\left(\dfrac{\partial \phi}{\partial y}\right) + \left(\dfrac{\partial \psi}{\partial x}\right)}} \\ \dfrac{d}{dz} f(z)\phi \\ \dfrac{d}{dz} f(z)\psi \end{pmatrix} \tag{2}$$

Where $\varepsilon = (\varepsilon_x \& \varepsilon_y)$ and $\gamma = (\gamma_{xz} \& \gamma_{yz})$ are the normal strains and shear strain transverse vectors, respectively, whereas ε_{xy} being in-plane strains. Table 1 shows the unique kinematic functions presented by different researchers and that by the present one. At the top and bottom surfaces, shear stresses should be zero, and this state is flawlessly satisfied with the present kinematic function contributed to developing nITSDT.

Table 1. Kinematic functions.

Kinematic function	Kirchhoff CPT	Mindlin FSDT	Reddy HSDT	Sayyad et al. SSNDT	Present nITSDT
$f(z) =$	0	z	$z - \frac{4}{3}\left(\frac{z^3}{h^2}\right)$	$\left(\frac{h}{\pi}\right) sin\left(\frac{\pi z}{h}\right)$	$cot^{-1}\left(\frac{h}{z}\right) - \left(\frac{16}{15}\right)\left(\frac{z}{h}\right)$

Constitutive Relations

It is able to capture expressions for stresses by substituting strains in the constitutive equation. Equation 3 describes the correlation between stresses and strains in the three axes directions.

$$\begin{Bmatrix} \sigma_x \\ \sigma_y \\ \tau_{xy} \\ \tau_{yz} \\ \tau_{xz} \end{Bmatrix} = \begin{bmatrix} Q_{11} & Q_{12} & 0 & 0 & 0 \\ & Q_{22} & 0 & 0 & 0 \\ & & Q_{66} & 0 & 0 \\ & Sym & & Q_{44} & 0 \\ & & & & Q_{55} \end{bmatrix} \begin{Bmatrix} \varepsilon_x \\ \varepsilon_y \\ \gamma_{xy} \\ \gamma_{yz} \\ \gamma_{xz} \end{Bmatrix} \tag{3}$$

where, Q_{ij} comprises the material stiffness coefficients shown in Eq. (4).

$$\left.\begin{matrix} Q_{11}, Q_{22} Q_{12} = \dfrac{E_1}{1 - \mu_{12}\mu_{21}}, \dfrac{E_2}{1 - \mu_{12}\mu_{21}} \dfrac{E_2}{1 - \mu_{21}} \\ Q_{66}, Q_{44} \qquad\qquad Q_{55} = G_{12}, G_{23} G_{13} \end{matrix}\right\} \tag{4}$$

where, in the direction of x, y and z the E_1, E_2, E_3 are the elasticity moduli. And, μ with Poisson's ratios with above notations, G_{12}, G_{13}, G_{23} are the shear moduli in the planes, respectively. Accordingly, the stress-strain relationships are definitive and are the basis for the stiffness/stress analyses of the plate exposed to a top surface transverse load.

Stress Resultants

Stress resultants are simplified representations of the stress state in the plate. The constitutive equations relating the stress resultants and the strains are expressed in Eq. (5).

$$\begin{bmatrix} N_i \\ M_i \end{bmatrix}_{6\times 1} = \begin{bmatrix} A_{ij} & B_{ij} \\ B_{ij} & D_{ij} \end{bmatrix}_{6\times 6} \begin{Bmatrix} \varepsilon_{0i} \\ k_i \end{Bmatrix}_{6\times 1} \tag{5}$$

The stiffness matrices are computed by integrating material stiffness coefficients as shown in Eq. (6),

$$A_{ij}^{(3\times3)} B_{ij}^{(3\times3)} D_{ij}^{(3\times3)} = \sum_{I}^{N} \int_{Zk-1}^{Zk} Q_{ij}(1, z, z^2) dz \tag{6}$$

where *i, j*=1, 2, 3.., and N, M is in-plane force and bending moments resultants respectively correspondingly termed as stress resultants shown in Figure 2, while A, B, D are extensional, coupling and bending moment stiffness matrices respectively, whereas ε_0 and k are membrane and curvature strains.

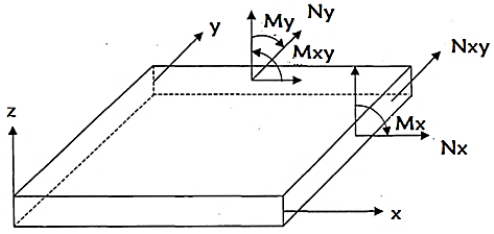

Figure 2. Force and moment resultants on a plate element.

Equation (7) shows a set of moment-curvature associations based on an implicit general stress field along the thickness derived by integrating the various stresses along with the depth of domain.

$$\begin{Bmatrix} N_x \\ N_y \\ N_{xy} \end{Bmatrix} = \int_{-\frac{h}{2}}^{\frac{h}{2}} \begin{Bmatrix} \sigma_x \\ \sigma_y \\ \tau_{xy} \end{Bmatrix} dZ, \quad \begin{Bmatrix} M_x \\ M_y \\ M_{xy} \end{Bmatrix} = \int_{-\frac{h}{2}}^{\frac{h}{2}} \begin{Bmatrix} \sigma_x \\ \sigma_y \\ \tau_{xy} \end{Bmatrix} Z \; dZ \quad \& \quad \begin{Bmatrix} P_{xz} \\ P_{yz} \end{Bmatrix} = \int_{-\frac{h}{2}}^{\frac{h}{2}} \begin{Bmatrix} \tau_{xz} \\ \tau_{yz} \end{Bmatrix} dZ \tag{7}$$

Equation (8) comprises the membrane and curvature strains.

$$\left.\begin{aligned} \varepsilon_{0i} &= \left(\varepsilon_x, \varepsilon_y, \gamma_{xy}\right)^T = \left(\frac{\partial u_0}{\partial x}, \frac{\partial v_0}{\partial y}, \frac{\partial u_0}{\partial y} + \frac{\partial v_0}{\partial x}\right)^T \\ k_i &= \left(\frac{\partial \phi}{\partial x}, \frac{\partial \psi}{\partial y}, \frac{\partial \phi}{\partial y} + \frac{\partial \psi}{\partial x}, 0, 0\right)^T \end{aligned}\right\} \tag{8}$$

Equilibrium Equations

Consider a plate domain of an elastic material. Inside the domain, Eq. (9) holds. The virtual work principle states equilibrium between the internal virtual work, δW_i and the external virtual work, δW_e in the configuration.

$$\left.\begin{aligned} &\delta W_i - \delta W_e = 0 \\ &\int_V \delta \varepsilon^T \sigma dv = \int_A \delta u^T p da \end{aligned}\right\} \tag{9}$$

Being, v the un-deformed volume, σ and $\delta\varepsilon$ the stress and virtual strain vector due to virtual displacement δu respectively with p being the surface traction acting over un-deformed area A. Equation (10) is then used to build the total virtual work.

$$\begin{aligned} &\int_A (\delta\varepsilon_x(N_x) + \delta\varepsilon_y(N_y) + \delta\gamma_{xy}(N_{xy}) + \delta\left(\frac{\partial\phi}{\partial x}\right)(M_x) + \delta\left(\frac{\partial\psi}{\partial y}\right)(M_y) + \delta\left(\frac{\partial\phi}{\partial y} + \frac{\partial\psi}{\partial x}\right)(M_{xy}) \\ &+\delta\gamma_{xz}(P_{xz}) + \delta\gamma_{xy}(P_{yz}))da \\ &= \int_S (\delta u_0(P_x) + \delta v_0(P_y))ds + \int_A \left(\delta w_0(q)\right)da \end{aligned} \tag{10}$$

The specified global edge tractions in the x and y directions are P_x and P_y, respectively, and q being the transverse load.

FINITE-ELEMENT MODEL

The internal and external virtual works can be only maintained, $\delta W_i = \delta W_e$ for a subset of fields of virtual displacement. This will lead to an approximate solution of the actual displacement field. In this sense, the virtual work principle is a weak statement of the equilibrium conditions. Finite element models (FE Model) is a way, as illustrated below, to build this subset of fields of virtual displacement.

i. Discretise the given domain using 8-noded serendipity finite elements as shown in Figure 3, being displacement vectors as variables at nodes. Serendipity elements are more efficient, and they avoid certain sorts of instabilities

since nodes are only added at the element boundary. They are sufficient to produce good agreements with low errors.

ii. Since the internal node is removed, this elimination results in a reduction in the size of the element matrices.

iii. Use Interpolate model for nodal and virtual nodal displacements through the elements.

iv. To express the virtual strain field in terms of virtual nodal displacements, control nodal strain-displacement relations (Eq. (2)) followed by using the nodal stress-strain relations (Eq. (3))

v. The maintenance $\delta W_i = \delta W_e$ of virtual nodal displacements for each set contributes to the solving of such algebraic equations.

Equilibrium Equations

A square plate with simply supported boundary conditions (SS-BCs) plate subjected to unit magnitude sinusoidal and uniformly distributed loads (SDL and UDL) is analysed assuming the Poisson ratio μ = 0.25 and 0.3. The geometrical information of the complete plate is square with side=1 and with S=4-100. The above symbolic characters are of standard meaning. One-quarter of the plate is evaluated as symmetry. Pre-processing is accompanied using a FEM Programme developed in MATLAB.

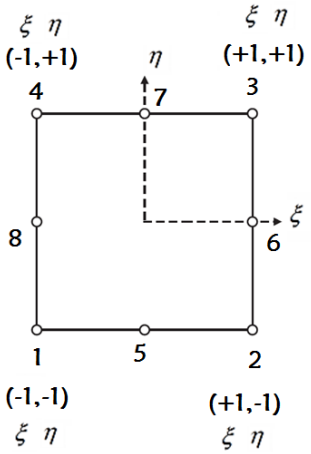

Figure 3. Simulated eight noded serendipity element Interpolation scheme.

This theory's FE approximation is based on the C^0 continuity. Equation 11 shows the displacement-vector:d inside the finite-element (FE) as a function of 8-distinct localities using shape functions (N_i).

$$(N_i) = \begin{bmatrix} (N_1) & 0 & (N_2) & 0 & -- & -- & -- & 0 \\ 0 & (N_1) & 0 & (N_2) & -- & -- & -- & (N_8) \end{bmatrix} \tag{11}$$

Shape functions and derivatives are requisites in strain calculations. Equation (12) shows the shape functions for the element illustrated in Figure 3 that are derived based on local coordinates "ξ &η" at a given node.

$$\left.\begin{array}{ll} N_1 = -0.25(1-\xi)(1-\eta)(1+\xi+\eta), & N_2 = 0.5(1-\xi)(1+\xi)(1-\eta) \\ N_3 = -0.25(1+\xi)(1-\eta)(1-\xi+\eta), & N_4 = 0.5(1+\xi)(1+\eta)(1-\eta) \\ N_5 = -0.25(1+\xi)(1+\eta)(1-\xi-\eta), & N_6 = 0.5(1-\xi)(1+\xi)(1+\eta) \\ N_7 = -0.25(1-\xi)(1+\eta)(1+\xi-\eta), & N_8 = 0.5(1-\xi)(1+\eta)(1-\eta) \end{array}\right\} \tag{12}$$

The displacement vector, $d_e$in the matrix form is an interpolation of nodal displacements, u_i, $v_i$etc., at a point in the element, as shown in Eq. (13).

$$d_e = \sum_{i=1}^{8} N_i \times \{u_i, v_i, w_i, \phi_i \, \&\psi_i\}^T \tag{13}$$

Combining Eq. (10) and Eq. (13), PVW equation $\chi(d)$ as shown in Eq. (14), is found in terms of global displacements and shape functions.

$$\begin{aligned} \chi(d) = & \int_A \{(B_0{}^T \times N_i) + (B_b{}^T \times M_i) + (B_s{}^T \times S)\} da \\ & \underbrace{- \int_A \{(B_N{}^T \times W_s) da)\} - \int_A \{(B_N{}^T \times W_e) ds)\}}_{\widetilde{Re}} \end{aligned} \tag{14}$$

where B_0, B_b, B_s, W_s, and W_e are namely in-plane, bending, transverse shear, transverse load and in-plane edge components. In addition, the successive iteration method is used to solve the assembled equilibrium equations (Eq. (14)). Assuming an error of 3 decimal and using the residual equation, Eq. (15), the solution is initialised. by imaginative $\chi(d)^i$ and K^T being tangent K matrix.

$$\left.\begin{array}{l} K^T = \left(\dfrac{\partial \chi(d.)^i}{\partial (d.)}\right) \\ (d.)^{i+1} = (d)^i + del(d)^i \\ \{\chi(d.)\}^{i+1} = \chi(d.)^i + K^T del(d.)^i \\ \left(\dfrac{(\chi^T \times \chi)}{({R_e}^T \times R_e)}\right) \le Error \end{array}\right\}. \tag{15}$$

The Gaussian Quadrature numerical integration scheme is shown by Eq. (16) for bending, and the membrane is 3×3 and that of transverse shear is 2×2.

$$I = \int_{-1}^{+1} fn(z)dz = \sum wN, kfn(xN, k) \tag{16}$$

where xN and wN are the sampling points and weights, respectively. The application of the reduced integration only to transverse shear terms with full integration kept for remaining terms resulted in the selective integration scheme. Table 2 shows the Gauss Legendre integration weights and sampling points.

Table 2. Gauss Legendre integration weights and sampling points.

Scheme	Two-point	Three-point
xN	$(-0.05773),\ (+0.05773)$	$(-0.7754),\ (0),\ (+0.7754)$
wN	$(1), (1)$	$(0.555), (0.888), (0.555)$

Illustrative Examples

Two examples are followed to validate the findings of the FE. Table 3 displays the material properties used on isotropic and transversely isotropic plates to achieve numerical results. The plate's upper surface is subjected to transverse load. As seen in Figure 4(a) and 4(b), the term q_0 reflects the load intensity at the plate midpoint, with *m* and *n* being odd numbers. The given transverse load is expanded in a double trigonometric Fourier series on the plate surface. The sinusoidal and uniformly distributed loads (SDL and UDL) are taken into account for plate study and shown in Table 4. Simply supported type of boundary conditions along all edges are associated for the plate, and the same is specified in Table 5.

Table 3. Material properties [10].

Examples	E_1	E_2	E_3	G_{12}	G_{13}	G_{23}	μ_{12}	μ_{13}	μ_{23}
Isotropic	1	1	1	0.38	0.38	0.38	0.3	0.3	0.3
Transversely isotropic	0.04	0.04	0.5	0.06	0.016	0.06	0.25	0.25	0.25

Table 4. Types of load.

Load	q	m, n
SDL	$\sum_{m}^{\infty}\sum_{n}^{\infty} q_0 \sin\left(\frac{m\pi}{a}\right)\sin\left(\frac{n\pi}{a}\right)$	1
UDL	$\sum_{m}^{\infty}\sum_{n}^{\infty} \frac{16q_0}{mn\pi^2}\sin\left(\frac{m\pi}{a}\right)\sin\left(\frac{n\pi}{a}\right)$	1, 3, 5…

Table 5. Boundary conditions.

BCs	Simply-supported (SS:BCs)
At y, x=0 ,a	$u_0 = w_0 = \psi = M_x = \dfrac{\partial w_0}{\partial x} = 0$
At x, y=0,b	$u_0 = w_0 = \phi = M_y = \dfrac{\partial w_0}{\partial y} = 0$

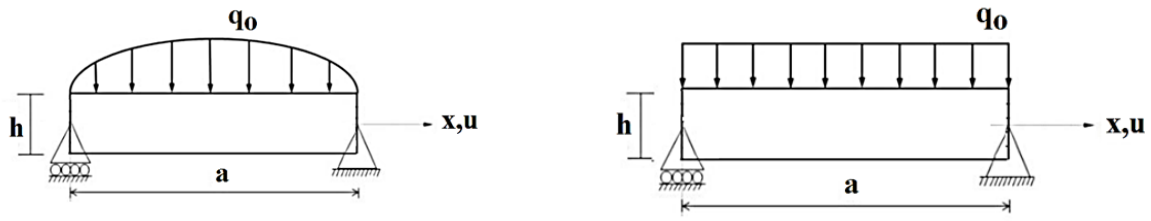

Figure 4. Load distribution on plate: (a) sinusoidal (SDL), and (b) uniform (UDL).

The displacements and stresses as shown in Eq. (17) to Eq. (19) are presented in the next non-dimensional forms that are widely presented in the prose for comparison and validation purposes. In MATLAB, a family of computer programmes has been written using the FEM formulation of nITSDT, a developed theory-of-plate for the linear bending analysis of plate structure. The organisation of the computer programmes established follows the standards introduced by Bathe [33] for the FEM algorithms. To promote the solution and reduce the computational time [28], the symbolic words in MATLAB are also implemented.

Transverse displacement:

$$\bar{w}_{\,at\,0} = \frac{10^2 w\,\mathrm{h}\,E_3}{q_0 S^3} \tag{17}$$

Normal stresses:

$$\bar{\sigma}_{x\ at\ \pm\frac{h}{2}} = \frac{\sigma_x}{q_0}\left(\frac{1}{S}\right)^2 \ \&\ \bar{\sigma}_{y\ at\ \pm\frac{h}{2}} = \frac{\sigma_y}{q_0}\left(\frac{h}{S}\right)^2 \tag{18}$$

Transverse stresses:

$$\bar{\tau}_{xy\ at\ \pm\frac{h}{6}} = \frac{\tau_{xy}}{q_0}\left(\frac{1}{S}\right)^2, \bar{\tau}_{xz\ at\ 0} = \frac{\tau_{xz}}{q_0}\left(\frac{1}{S}\right) \ \&\ \bar{\tau}_{yz\ at\ 0} = \frac{\tau_{yz}}{q_0}\left(\frac{1}{S}\right) \tag{19}$$

RESULTS AND DISCUSSION

Mesh-Convergence Study

The mesh-convergence comparative analysis in non-dimensional transverse displacement results was obtained in [10] and [16], and the sample case of the present analysis is in Table 6. The results using a free mesh show that the mesh size (10 ×10) is converged and has an excellent correlation with benchmark results [16]. The equilibrium equations are solved using an Iterative method with a convergence tolerance of three decimals. All the illustrative examples and cases are solved by mesh size (10×10), and these are discussed in the preceding section.

Table 6. Convergence study on non-dimensional transverse displacements $\bar{w}$ for isotropic plate subjected to SDL.

S	Approach	Hypothesis	$\bar{w}$
	Analytical	[10]	3.6534
	Exact	[16]	3.6630
		Mesh size	
4		4×4	3.6789
	FEM Present	6×6	3.66354
		8×8	3.66312
		10×10	3.66312

Bi-directional Bending Analyses: Isotropic Plates

The efficacy of nITSDT's in bending analysis of thick to thin isotropic plates under SDL/UDL loadings is demonstrated in this section. Properties of the isotropic material described in Table 3 are referred. The non-dimensional central-displacement, in-plane/transverse-stresses through the thickness subjected to SDL with different side-to-thickness (S=a/h) ratios are presented in Table 7. The outcomes obtained are contrasted with the analytical solution [10] and the exact elasticity result [16].

Table 8 shows non-dimensional central displacements, in-plane stresses, and transverse stresses as a function of plate thickness with different values of S subjected to UDL. The model is verified to the analytical solution [10] and exact solution [16]. Table 7 and Table 8 also shows the per cent of errors computed for non-dimensional central displacements, in-plane stresses, and transverse stresses. For example, in Table 7, the per cent error for non-dimensional central displacements at S=4 may simply estimate that this error is 0.0027 for the current work, which is smaller than 0.2620 for other researchers. Examination of Table 7 and Table 8 show this new theory estimates the displacements correctly while overestimating the normal in-plane stresses for thick to thin plates. In the literature, there are no exact outcomes for in-plane shear stresses. When utilising constitutive relations, the current hypothesis overvalues the values of transverse shear stresses, but once employing equations of equilibrium from the elasticity theory, it appropriately predicts such stresses.

Table 7. Isotropic square plate subjected to SDL: Non-dimensional central displacements and stresses.

S	Hypothesis	Model	$\bar{w}$ $(0.)$	%-Error	$\bar{\sigma}_x \& \bar{\sigma}_y$ $\left(-\frac{h}{2}.\right)$	%-Error	$\bar{\tau}_{xy}$ $\left(-\frac{h}{2}.\right)$	$\bar{\tau}_{xz} \& \bar{\tau}_{yz}$ $(0.)$	%-Error
4	Present.	nITSDT	3.6631	0.0027	0.2102	3.0392	0.1118	0.2392	1.3130
	[10]	SSNDT	3.6534	0.2620	0.2267	11.127	0.1063	0.2444	3.515
	[16]	Exact	3.6630	0	0.2040	0	–	0.2361	0
10	Present.	nITSDT	2.9742	1.0773	0.2003	0.7545	0.1065	0.2401	0.7553
	[10]	SSNDT	2.9333	0.3126	0.2125	6.8913	0.1060	0.2454	2.9794
	[16]	Exact	2.9425	0	0.1988	0	–	0.2383	0
20	Present.	nITSDT	2.8342	0.12334	0.1988	0.4547	0.1058	0.2426	1.6764
	[10]	SSNDT	2.8286	0.32061	0.2105	6.3668	0.1060	0.2455	2.8918
	[16]	Exact	2.8377	0	0.1979	0	–	0.2386	0
50	Present.	nITSDT	2.8108	0.0925	0.1984	0.4048	0.1055	0.2403	0.7124
	[10]	SSNDT	2.7991	0.3240	0.2100	6.2753	0.1060	0.2456	2.9337
	[16]	Exact	2.8082	0	0.1976	0	–	0.2386	0
100	Present.	nITSDT	2.8060	0.0713	0.1984	0.4048	0.1055	0.2403	0.6702
	[10]	SSNDT	2.7949	0.3245	0.2099	6.2246	0.1060	0.2456	2.8906
	[16]	Exact	2.8040	0	0.1976	0	–	0.2387	0

Table 8. Isotropic square plate subjected to UDL: Non-dimensional central displacements and stresses.

S	Hypothesis	Model	$\bar{w}$ $(0.)$	%-Error	$\bar{\sigma}_x \& \bar{\sigma}_y$ $\left(-\frac{h}{2}.\right)$	%-Error	$\bar{\tau}_{xy}$ $\left(-\frac{h}{2}.\right)$	$\bar{\tau}_{xz} \& \bar{\tau}_{yz}$ $(0.)$	%-Error
4	Present.	nITSDT	5.7047	0.1756	0.3008	2.0352	0.2194	0.4751	3.1480
	[10]	SSNDT	5.6799	0.2591	0.3185	8.0393	0.2082	0.4833	4.9283
	[16]	Exact	5.6947	–	0.2948	–	–	0.4606	–
10	Present	nITSDT	4.6376	0.0452	0.2980	3.2571	0.1978	0.4857	0.2874
	[10]	SSNDT	4.6252	0.3125	0.3071	6.4102	0.1954	0.5044	3.5516
	[16]	Exact	4.6397	–	0.2886	–	–	0.4871	–
20	Present.	nITSDT	4.4832	0.0869	0.3011	4.6940	0.1943	0.4977	0.9328
	[10]	SSNDT	4.4727	0.3209	0.3054	6.1891	0.1942	0.5083	3.0825
	[16]	Exact	4.4871	–	0.2876	–	–	0.4931	–
50	Present.	SSNDT	4.4499	0.1282	0.2950	2.6443	0.1941	0.4947	0.0202
	[10]	nITSDT	4.4644	0.4545	0.3132	8.9770	0.1933	0.4983	0.7480
	[16]	Exact	4.4442	–	0.2874	–	–	0.4946	–
100	Present.	nITSDT	4.4377	0.0090	0.2830	1.4966	0.1932	0.4950	0.0202
	[10]	SSNDT	4.4238	0.3221	0.3049	6.1260	0.1941	0.5092	2.8894
	[16]	Exact	4.4381	–	0.2873	–	–	0.4949	–

Figure 5 displays the surface plot of bending of the mid-plane of an isotropic plate subjected to SDL. For a few cases, this has been plotted. But a case of SDL with S=4 is pursued only to see the nature of the bending behaviour of the plate. From the nature and results reported on it, the peak value of non-dimensional $\bar{W}$is 3.6631 at the centre of the plate, and the same is seen in Table 7. For SDL and UDL, Figure 6 displays the non-dimensional central deflection $\bar{w}$ versus length-thickness ratio (a/h). The variation of $\bar{w}$ for a/h=4, 6, 8, 10, 14, 20, 50 and 100 is very precise. The value of $\bar{w}$ of UDL for all a/h is approximately 1.5 times greater than that of SDL. This is due to UDL is constant over the top surface of plate.

Figure 7 depicts in-plane normal stress, $\bar{\sigma}_x$ variations as a function of thickness at S=4 for both SDLand UDL. The behaviour of this plot is accurate when compared with renowned literature. Here also maximum non-dimensional$\bar{\sigma}_x$ for UDL is 1.5 times more than that of SDL because the former is at constant load over the surface. Figure 7(a) to Figure (c) illustrate the through thickness in-plane normal stress $\bar{\sigma}_x$, in-plane shear stress $\bar{\tau}_{xy}$, and transverse shear stress $\bar{\tau}_{xz}$, respectively. These plots are drawn at S=4 for both SDL and UDL. The behaviour of these plots is accurate when compared with renowned literature. Here also, maximum non-dimensional stresses for UDL are 1.5 to 2 times more than that of SDL because the former is at constant load over the surface.

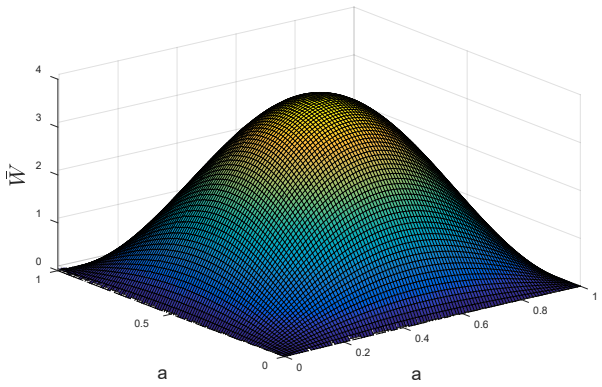

Figure 5. Surface plot for transverse bending of mid-plane of an isotropic plate subjected to SDL at S=4, (maximum $\bar{W}$=3.6698, Table 1).

The through thickness $\bar{\tau}_{xz}$and transverse shear stress plots of SDL for S=4, 10, 20, 50 and 100 are shown in Figure 8. The behaviour of these curves show a small difference in the maximum value of $\bar{\tau}_{xz}$ at mid-plane of the plate. Thus, increasing S more than 25 becomes redundant. The superlative results are found in the thick plate than that of the thin one.

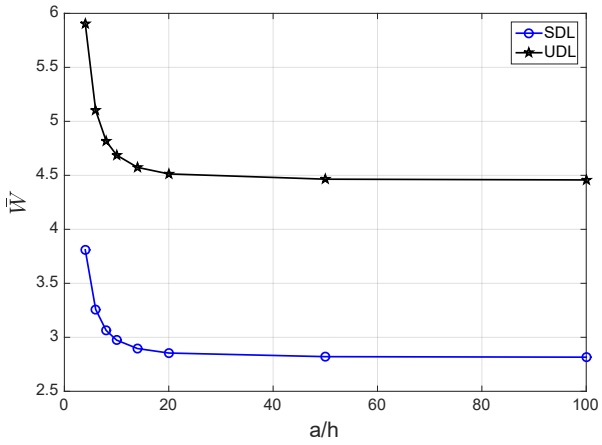

Figure 6. Surface plot comparison of non-dimensional central deflection $\bar{w}$ versus length–thickness ratio(a/h).

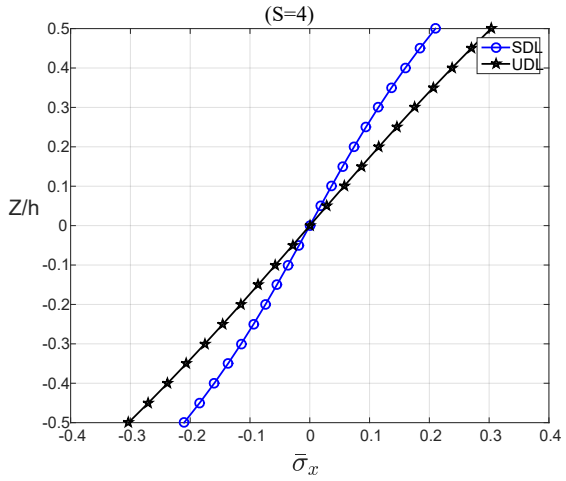

(a) non-dimensional in-plane normal stress $\bar{\sigma}_x$

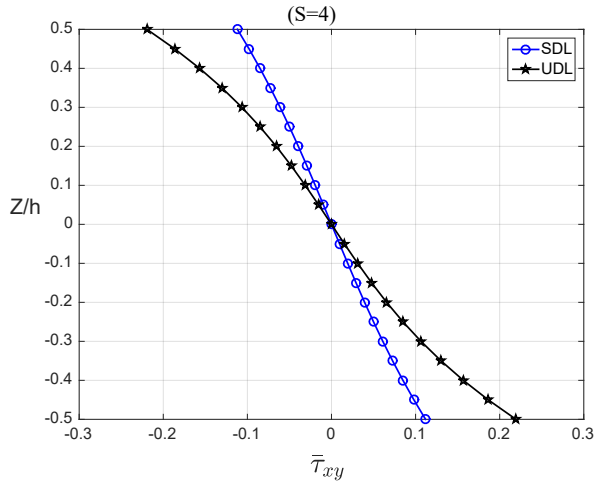

(b) non-dimensional in-plane shear stress normal stress $\bar{\tau}_{xy}$

(S=4).

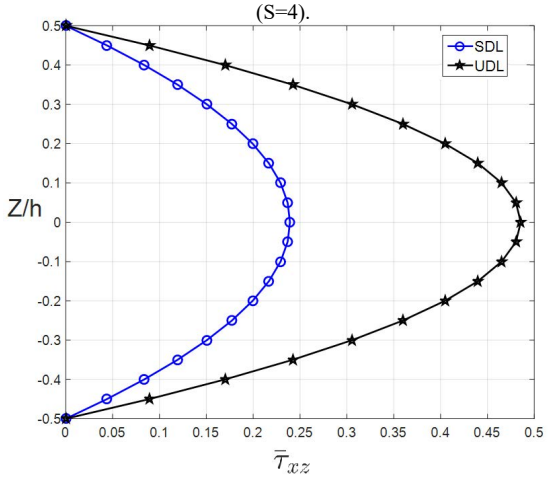

(c) non-dimensional transverse shear stress $\bar{\tau}_{xz}$

Figure 7. Isotropic square plate subjected to UDL and UDL.

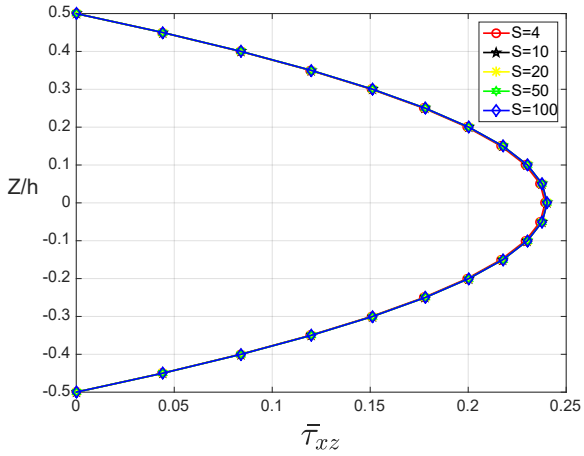

Figure 8. Isotropic and transversely isotropic plates subjected to SDL: Non-dimensional transverse shear stress $\bar{\tau}_{xz}$ (S=4-100).

Bi-directional Bending Analysis: Transversely Isotropic Plates

The efficacy of the present hypothesis for the bi-directional bending in transversely isotropic plates under SDL/UDL is validated in this section. Properties of the material described in Table 3 are included. Table 9 and Table 10 present the non-dimensional central displacements, in-plane/transverse stresses through the depth in plates with different values of S subjected to SDL and UDL. Because an exact-elasticity solution is not accessible in the literature, the findings obtained are compared to an analytical solution by SNDT[10], HSDT[5], FSDT[4] and CPT[1], and these are included in Table 9 and Table 10. The findings obtained by current theory and by HSDT [5] are almost the same. While, results in [1] and [5] appears similar at the highest value of S.

Table 9. Non-dimensional displacements and stresses: Transversely-isotropic plate subjected to SDL.

S	Hypothesis	Model	$\bar{w}$ (0.)	% Error	$\bar{\sigma}_x \& \bar{\sigma}_y$ $\left(-\frac{h}{2}.\right)$	%-Error	$\bar{\tau}_{xy}$ $\left(-\frac{h}{2}.\right)$	$\bar{\tau}_{xz} \& \bar{\tau}_{yz}$ (0.)	%-Error
4	Present.	nITSDT	38.954	0.00514	0.1936	0.05163	0.1149	0.2378	0.0420
	[10]	SNDT	39.146	0.49933	0.1936	0.05163	0.1153	0.2377	0.0840
	[5]	HSDT	38.952	0	0.1937	0	0.1147	0.2379	0
	[4]	FSDT	39.257	0.7850	0.1900	1.9101	0.1140	0.2387	0.3362
	[1]	CLPT	36.091	7.3638	0.1900	1.9101	0.1140	0.2387	0.3362
10	Present.	nITSDT	36.307	0.0330	0.1912	0.1044	0.1138	0.2387	0.0418
	[10]	SSNDT	36.578	0.7797	0.1909	0.2612	0.1142	0.2385	0.0419
	[5]	HSDT	36.295	0	0.1914	0	0.1133	0.2386	0
	[4]	FSDT	36.598	0.83482	0.1900	0.7314	0.1140	0.2388	0.0410
	[1]	CLPT	36.091	0.56206	0.1900	0.7314	0.1140	0.2389	0.0411

Table 10. Non-dimensional displacements and stresses: Transversely-isotropic plate subjected to UDL.

S	Hypothesis	Model	$\bar{w}$ $(0.)$	%-Error	$\bar{\sigma}_x \& \bar{\sigma}_y$ $\left(-\frac{h}{2}.\right)$	%-Error	$\bar{\tau}_{xy}$ $\left(-\frac{h}{2}.\right)$	$\bar{\tau}_{xz} \& \bar{\tau}_{yz}$ $(0.)$	%-Error
4	Present.	nITSDT	61.289	0.0636	0.2805	0.0356	0.2179	0.4917	2.1073
	[10]	SSNDT	61.577	0.5338	0.2803	0.1069	0.2180	0.4686	2.6993
	[5]	HSDT	61.250	0	0.2806	0	0.2178	0.4816	0
	[4]	FSDT	61.732	0.7869	0.2763	1.53243	0.2086	0.4951	2.7823
	[1]	CLPT	57.127	6.7313	0.2763	1.5324	0.2086	0.4951	2.7823
10	Present	nITSDT	57.403	0.0313	0.2781	0.0359	0.2113	0.4925	0.0405
	[10]	SSNDT	57.835	0.7841	0.2775	0.2516	0.2098	0.4917	0.2029
	[5]	HSDT	57.385	0	0.2782	0	0.2136	0.4927	0
	[4]	FSDT	57.864	0.8347	0.2763	0.6829	0.2086	0.4951	0.4668
	[1]	CLPT	57.127	0.4495	0.2763	0.6829	0.2086	0.4951	0.4668

Table 9 and 10 also show the per cent of errors computed for central displacements, in plane stresses, and transverse stresses. For example, Table 8 shows that the per cent error for transverse shear stresses at S=4 is 0.0420, which is smaller than the 0.0840 and 0.3362 reported by other researchers. The in-plane normal stress $\bar{\sigma}_x$ through thickness in the transversely isotropic plate is shown in Figure 9(a). Also in Figure 9(b) displays the evaluation of in-plane normal stresses $\bar{\sigma}_x$ for through thickness in isotropic and transversely isotropic at S=4. All these behaviour of these plots are accurate when compared with prominent literature. Here also the maximum value of $\bar{\sigma}_x$ for isotropic plate is around 1.2 times than that of transversely isotropic. Similarly, comparison of through thickness in-plane shear stress $\bar{\tau}_{xy}$ for the isotropic and transversely isotropic plate at S=4 is shown in Figure 10. The maximum value of $\bar{\tau}_{xy}$ for isotropic plate is around two times than that of transversely isotropic. This is due to the more bending stiffness of isotropic material than that of transversely isotropic material plate.

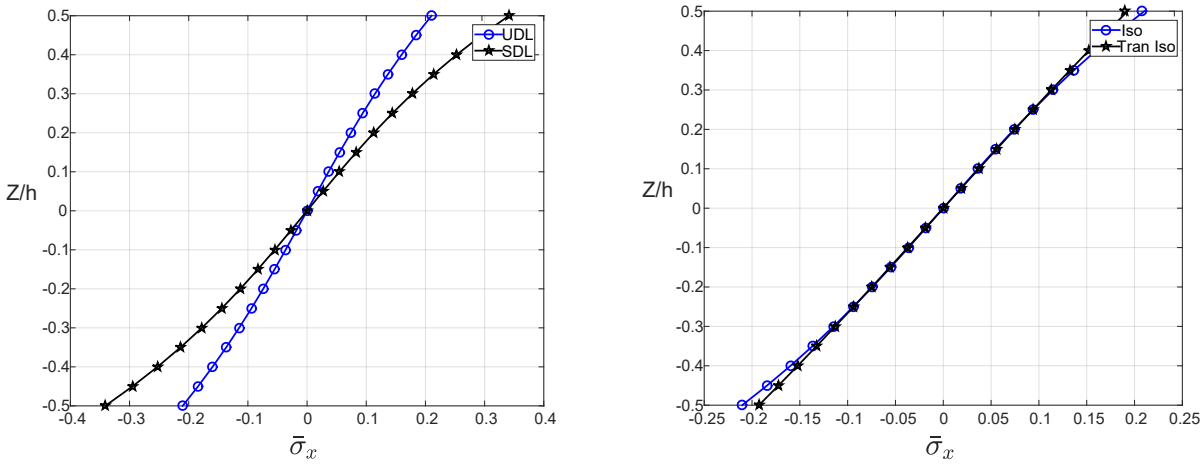

(a) Transversely isotropic-plate subjected to SDL/UDL (b) isotropic/ transversely isotropic plate subjected SDL

Figure 9. Non-dimensional in-plane normal stress $\bar{\sigma}_x$ (S=4).

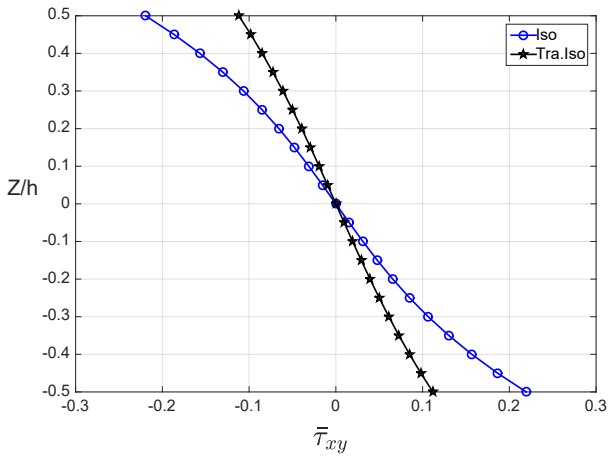

Figure 10. Non-dimensional in-plane shear stress $\bar{\tau}_{xy}$: Isotropic/ transversely isotropic plate subjected SDL (S = 4).

CONCLUSION

The finite element formulation for bending analysis of isotropic and transversely isotropic plate has been developed based on a new inverse trigonometric shear deformation theory (nITSDT. The implications of both transverse-shear and normal-shear deformations are considered in this theory. In-plane and transverse deformations use an inverse trigonometric shape function expanded to account for the effects of transverse shear and normal deformations. This theory does not need a problem-dependent shear correction factor since it uses constitutive relationships to satisfy traction free boundary conditions at the top and bottom surfaces of the plate. Using FE based MATLAB solution method, the plate is analysed for simply supported-boundary conditions. The combination of numerical and symbolic aspects of the problem-solving method is also important, as MATLAB has proven to be a flexible software that allows numerical and symbolic computation to be combined. It is inferred from the computational analysis and discussion of findings that the current theory, when compared to other HSDTs for Isotropic and transversely isotropic plates available in the literature, yields precise predictions of displacements and stresses. For all loading instances, the findings of displacements and stresses derived by this theory are in great agreement with those obtained by precise solutions.

ACKNOWLEDGEMENT

The authors would like to thank Sanjivani College of engineering Kopargaon, SP Pune University, Pune, India for providing facility research software lab to complete this work.

REFERENCES

[1] G. R. Kirchhoff, "U¨ ber das Gleichgewicht und die Bewegung einer elastischen Scheibe," *Journal fu¨r die reine und angewandte Mathematik*, vol. 40, pp. 51-88, 1850, doi.org/10.1515/crll. (in German).

[2] E. Reissner, "The effect of transverse shear deformation on the bending of elastic plates," *J. Appl. Mech.*, vol. 12, pp.69-77, 1945, doi.org/10.1177/002199836900300316.

[3] R. D. Mindlin, "Influence of rotatory inertia and shear on flexural motions of isotropic elastic plates," J. Appl. Mech., vol. 18, pp. 31-38, 1951. doi.org/10.1115/1.4010217.

[4] M. Kashtalyana, R. Kienzlerb, and M. Meyer-Coorsb, "Development of the consistent second-order plate theory for transversely isotropic plates and its analytical assessment from the three-dimensional perspective," *Thin-Walled Struct.*, vol. 163, pp.1-12, 2021, doi.org/10.1016/j.tws.2021.107704.

[5] J. N. Reddy, "A simple higher order theory for laminated composite plates," *J. Appl. Mech.*, vol.51,no.4,pp.745-752, 1984, doi:10.1115/1.3167719.

[6] A. K. Noor and W. S. Burton, "Assessment of shear deformation theories for multilayered composite plates," *Appl. Mech. Rev.*, vol. 42, no.1, pp.1-13, 1989, doi:10.1115/1.3152418.

[7] P. V. Avhad and A. S. Sayyad, "Static analysis of functionally graded composite beams curved in elevation using higher order shear and normal deformation theory," *Mater. Today: Proc.,* vol. 21, no.2, pp. 1195-1199, 2020, doi.org/10.1016/j.matpr.2020.01.069

[8] E. Carrera, "An assessment of mixed and classical theories for the thermal stress analysis of orthotropic multilayered plates, " *J. Therm. Stresses*, vol. 23, no.8, pp.797–831, 2020. doi:10.1080/014957300750040096.

[9] Y. M. Ghuga and R. P. Shimpi, "A review of refined shears deformation theories for isotropic and anisotropic laminated plates," *J. Reinf. Plast. Compos*, vol. 21, no. 9, pp. 775–813, 2002, doi: 10.1177/073168402128988481.

[10] A. S. Sayyad and Y. M. Ghugal, "A new shear and normal deformation theory for isotropic, transversely isotropic, laminated composite and sandwich plates," *Int. J. Mech. Mater. Des,* vol. 10, no. 3, pp. 247–267, 2014, doi:10.1007/s10999-014-9244-3.

[11] R. P. Shimpi and H. G. Patel, "A two variable refined plate theory for orthotropic plate analysis," *Int. J. Solids Struct.*, vol. 43, no. 22-23, pp. 6783-6799, 2006, doi.org/10.1016/j.ijsolstr.2006.02.007.

[12] F. Yue *et al.*, "Bending analysis of circular thin plates resting on elastic foundations using two modified vlasov models," *Math. Probl. Eng*, vol. 2020, pp.1–12. 2020. doi:10.1155/2020/2345347.

[13] A. S. Sayyad and Y. M. Ghugal, "Static and free vibration analysis of laminated composite and sandwich spherical shells using a generalised higher-order shell theory," *Compos. Struct*, vol. 219, pp. 129–146, 2019. doi.org/10.1016/j.compstruct.2019.03.054.

[14] N. J. Pagano, "Exact solutions for bidirectional composites and sandwich plates," *J. Compos. Mater.*, vol. 4, pp. 20-34, 1970, doi.org/10.1177/002199837000400102.

[15] S. Srinivas, C. V. Joga Rao, and A. K. Rao, "An exact analysis for vibration of simply supported homogeneous and laminated thick rectangular plates," *J. Sound Vib*, vol. 12, no. 2, pp.187-199, 1970, doi.org/10.1016/0022-460X(70)90089-1.

[16] A.M. Zenkour, "The effect of transverse shear and normal deformations on the thermo-mechanical bending of functionally graded sandwich plates," *Int. J. Appl. Mech.*, vol. 1, no. 14, pp. 667–707, 2009, doi.org/10.1142/S1758825109000368.

[17] Y M Ghugal and P D. Gajbhiye, "Bending analysis of thick isotropic plates by using 5th order shear deformation theory," *J. Appl. Comput. Mech.*, vol. 2, no. 2, pp. 80-95, 2016, doi: 10.22055/JACM.2016.12366.

[18] E. Reissner, "On the theory of bending of elastic plates," *J. Math. Phys.*, vol. 23, pp. 184-191, 1944, doi.org/10.1002/sapm1944231184.

[19] G. Samadi, B. N. Neya, and Parvaneh Nateghi Babag, "Bending analysis of transversely isotropic thick rectangular plates on two-parameter elastic foundation,"*J. Civ. Environ. Eng.*, vol. 49, no. 3, pp. 53-64, 2019, magiran.com/p2057678.

[20] B. Woodward and M. Kashtalyan, "Three-dimensional elasticity analysis of sandwich panels with functionally graded transversely isotropic core," *Arch. Appl. Mech*, vol. 1, pp. 1-22, 2019, doi:10.1007/s00419-019-01589-y.

[21] F. Yekkalam, Tash, and B. N. Neya, "An analytical solution for bending of transversely isotropic thick rectangular plates with variable thickness, "*Appl. Math. Model*, vol. 77, no. 2,pp 1582-1602, 2020, doi.org/10.1016/j.apm.2019.08.017.

[22] D. P. Bhaskar and A. G. Thakur, "FE modeling for geometrically nonlinear analysis of laminated plates using a new plate theory," *Adv. Aircr. Spacecr. Sci*, vol. 6, no. 5, pp. 409-426, 2019, doi.org/10.12989/aas.2019.6.5.409.

[23] D. Bhaskar and A. Thakur, "Geometrically nonlinear analysis of laminated composite plates subjected to uniform distributed load using a new hypothesis: the finite element method (FEM) approach," *Mech. Adv. Compos. Struct*, vol. 7, pp. 271-285, 2020, doi:10.22075/MACS.2020.18572.1222.H.

[24] N. S. Naik and A. S. Sayyad, "An accurate computational model for thermal analysis of laminated composite and sandwich plates," *J. Therm. Stress*, vol. 42, no. 5, pp. 559–579, 2019, doi.org/: 10.1080/01495739.2018. 1522986..

[25] A. S. Sayyad and Y. M. Ghugal, "On the free vibration analysis of laminated composite and sandwich plates: a review of recent literature with some numerical results," *Compos. Struct*, vol. 129, pp. 177–201, 2015, doi.org/10.1016/j.compstruct.2015.04.007.

[26] A. S. Sayyad and Y. M. Ghugal, "Bending, buckling and free vibration of laminated composite and sandwich beams: a critical review of literature," *Compos. Struct*, vol. 171, pp. 486–504, 2017, doi.org/ 10.1016/j. compstruct.2017.03.053.

[27] M. G. Rivera and J. N. Reddy, "Nonlinear transient and thermal analysis of functionally graded shells using a seven parameter shell finite element," *J Model. Mech. Mater Mod.*, vol. 1, no. 2, pp. 20170003, 2017, doi.org/10.1515/jmmm-2017-0003.

[28] E. Carrera, "An assessment of mixed and classical theories for the thermal stress analysis of orthotropic multilayered plates," *J. Therm. Stress*, vol. 23, no. 9, pp. 797–831, 2000, doi.org/10.1080/014957300750040096.

[29] E. Carrera *et al.*, "Results on best theories for metallic and laminated shells including layer-wise models," *Compos. Struct*, vol. 126, pp. 285–298, 2015, doi.org/10.1016/j.compstruct.2015.02.027.

[30] E. Carrera and S. Valvano, "A variable kinematic shell formulation applied to thermal stress of laminated structures," *J. Therm. Stress*, vol. 40, no. 7, pp. 803–827, 2017, doi.org/10.1080/01495739.2016.1253439.

[31] A. S. Sayyad, Y. M. Ghugal, and B. A. Mhaske, "A four-variable plate theory for thermoelastic bending analysis of laminated composite plates," *J. Therm. Stress*, vol. 38, no. 8, pp. 904–925, 2015, doi.org/ 10.1080/ 01495739.2015.1040310.

[32] C. M. C. Roque, "Symbolic and numerical analysis of plates in bending using Matlab," *J. Symb. Comput*, vol. 61, no. 62, pp. 3-11, 2014, doi.org/10.1016/j.jsc.2013.10.005.

[33] X. Wang and G. Shi, "A simple and accurate sandwich plate theory accounting for transverse normal strain and interfacial stress continuity," *Compos. Struct*, vol. 107, pp. 620–628, 2014, doi:10.1016/j.compstruct.2013.08.033.